

A simple photoacoustic method for the in situ study of soot distribution in flames

G. S. Humphries^{1,2} · J. Dunn¹ · M. M. Hossain¹ · M. Lengden² · I. S. Burns¹ · J. D. Black¹

Received: 14 November 2014 / Accepted: 11 April 2015
© The Author(s) 2015. This article is published with open access at Springerlink.com

Abstract This paper presents a simple photoacoustic technique capable of quantifying soot volume fraction across a range of flame conditions. The output of a high-power (30 W) 808-nm cw-diode laser was modulated in order to generate an acoustic pressure wave via laser heating of soot within the flame. The generated pressure wave was detected using a micro-electro-mechanical microphone mounted close to a porous-plug flat-flame burner. Measurements were taken using the photoacoustic technique in flames of three different equivalence ratios and were compared to laser-induced incandescence. The results presented here show good agreement between the two techniques and show the potential of the photoacoustic method as a way to measure soot volume fraction profiles in this type of flame. We discuss the potential to implement this technique with much lower laser power than was used in the experiments presented here.

1 Introduction

Soot and condensed-phase hydrocarbons generated by the incomplete combustion of organic fuels have recently been shown to be a significant contributing factor in global climate change [1]. Atmospheric soot levels have also been shown to have detrimental effects on health [2]. The development of accurate measurement techniques for the study

of soot formation during combustion is a key step in developing soot reduction strategies [3, 4].

Optical measurement techniques are ideally suited for combustion environments because they generally cause negligible perturbation to the combustion process. One of the most widely used optical techniques for the study of particulate matter in flames is laser-induced incandescence (LII). Typical LII experimental schemes use a high-power pulsed laser source (such as a solid-state Nd:YAG laser) [5] to heat the soot particles. The resulting thermal emission is then detected, usually over a narrow range of wavelengths selected using either a system of optical filters [6] or a monochromator [7]. The peak signal level provides a measure of the relative soot volume fraction. The absolute soot volume fraction is found either by calibration based on optical extinction measurements [8, 9] or by a two-colour approach in which a second filtered detector collects light from the same measurement volume, and the ratio of signals is used to determine the peak particle temperature [10, 11]. A feature of this type of experimental set-up is that a high-power pulsed laser source and relatively fast photodetectors or intensified cameras are required.

Photoacoustic (PA) detection has been used to make highly sensitive laser absorption measurements in a number of applications, such as IR spectroscopy [12]. The principle of photoacoustic detection of particles is that absorption of the incident laser energy leads to an increase in the temperature of the particle. Heat is transferred from the particles to the surrounding gas, resulting in the expansion of the gas [13]. A change in laser intensity leads to a change in the rate of heat transfer, and an acoustic pressure wave can therefore be established by modulating the intensity of the laser [14]. The pressure wave can be detected using a microphone, and its amplitude measured using a lock-in amplifier. This method of detection has a further advantage

✉ I. S. Burns
iain.burns@strath.ac.uk

¹ Department of Chemical and Process Engineering, University of Strathclyde, Glasgow G1 1XJ, UK

² Department of Electronic and Electrical Engineering, University of Strathclyde, Glasgow G1 1XW, UK

over purely optical systems, in that it is immune from any interference from background radiation, since the photoacoustic signal gives a direct measurement of the proportion of light absorbed [15]. Photoacoustic detection using acoustically resonant cells has been applied to quantify low concentrations of particulate matter in ambient air [16] and in vehicle exhaust emissions [17], but there have been few applications of photoacoustic detection to flames or combustion processes.

The use of an acoustically resonant cell provides amplification of the acoustic signal which yields higher sensitivity without increasing the laser power or modulation depth. One of the disadvantages of this approach is that the modulation frequency of the laser must match an acoustic resonant mode of the cell. This limitation, however, can be overcome by careful cell design [18]. Construction of a high-quality acoustic resonant cell around a burner would be difficult as the acoustic resonance is hampered by temperature gradients in and around the flame. Using a photoacoustic detection scheme without such a cell requires a significantly higher laser power to achieve equivalent sensitivity [19]. There have been a few studies using a flash-lamp-pumped dye laser with photoacoustic detection, measuring sodium seeded in a flame by scanning the dye laser through the sodium D-line absorption [20] and measuring low concentrations of NO_2 in a flame [21]. Rose and Gupta used related methods, photoacoustic deflection and photothermal deflection in a sooting acetylene flame [22] where the deflection of a flash-lamp-pumped dye laser beam, or deflection of a HeNe laser probe beam due to pressure variations induced by the dye laser, was measured. Nevertheless, these studies were based on high-power pulsed lasers so a different methodology is required to achieve a simple, compact and inexpensive instrument.

Continuous-wave diode lasers capable of high output powers (typically around 30–50 W) have become readily available in recent years. However, their application to measurements in the combustion environment has been somewhat limited. We present in this paper a simple photoacoustic technique for in situ quantification of soot in flames. Our technique does not employ any acoustic resonator, allows for the use of relatively inexpensive diode laser sources and utilises a small inexpensive micro-electro-mechanical (MEMS) microphone.

2 Experimental set-up

The experimental set-up used for photoacoustic detection is shown in Fig. 1. A fibre-coupled, high-power (30 W) continuous-wave diode laser ($\lambda = 808$ nm, DiLAS) was used to thermally excite soot particles formed in a laminar, premixed ethylene/air flame stabilised on a porous-plug

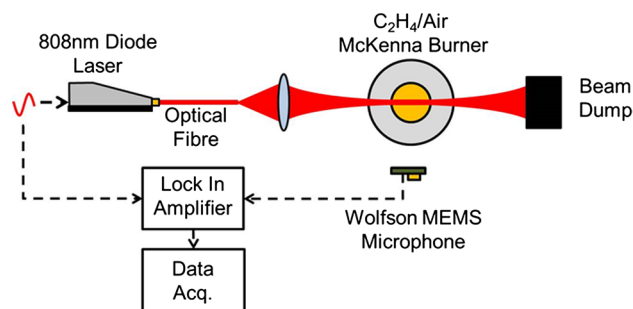


Fig. 1 Experimental set-up for photoacoustic soot measurement

burner. The light emitted from the 600- μm multi-mode fibre was focused using a plano-convex lens (focal length 120 mm), resulting in a measured $1/e^2$ beam diameter of 1.06 mm at the centre of the burner. A thermal laser power meter was used to monitor the intensity of the transmitted beam. The laser power was modulated sinusoidally at 10 kHz by supplying a modulated control voltage from a function generator to the laser drive electronics which in turn modulated the current supplied to the laser diode. The resulting intensity modulation produced an acoustic wave when absorption was present that was then detected using a MEMS microphone (Wolfson Microelectronics) located 60 mm from the burner centreline. The microphone is sensitive over a wide range of frequencies, and a broadband acoustic measurement would be highly susceptible to background noise. Instead, a lock-in amplifier (Stanford Research Systems, SRS 830) was used to detect the acoustic signal at the modulation frequency of 10 kHz. A relatively high modulation frequency of 10 kHz was chosen because the power spectral density of ambient sound is expected to be roughly inversely proportional to frequency. The lock-in amplifier acts as a narrow band-pass filter and has the effect of suppressing any noise that is not at the modulation frequency. The time constant of the lock-in amplifier was set to 3 s. Measurements were digitised using a data acquisition card and were averaged for a period of 10 s. The amplitude of the laser modulation was approximately 130 mW with a mean output power of 15.5 W.

A high-power laser was used because it was initially thought that a large modulation amplitude might be required to achieve the required sensitivity. In fact, the modulation amplitude was limited by the frequency response of the available drive electronics and the laser diode itself. It was found, however, that this modulation amplitude was sufficient to make useful measurements. The use of an optical chopper was initially investigated as a means of producing a higher modulation depth, but difficulties were encountered in achieving a sufficiently high modulation frequency. Additional noise was observed, and this was attributed to unstable photoacoustic effects

generated at the detection frequency due to the laser heating the chopper blades.

The transverse profile of the laser beam was measured at several points along the beam path by translating a knife edge through the beam. The beam was measured to have a near-Gaussian intensity distribution. Although focused at the centre of the flame, the beam waist was nearly constant over the burner diameter, expanding out to a $1/e^2$ beam diameter of 1.30 mm at the extremities of the flame.

The burner employed for this work used a stainless steel porous plug to produce a one-dimensional flame, with conditions varying only as a function of height above the burner. The premixed gas flow rates were based on the standard reference flame defined by the International LII Workshop [23] and the International Sooting Flame Workshop [24], but the flow rates were modified to maintain the specified mass flux for our burner which has a smaller plug diameter of 33 mm. The burner is water-cooled, and the flame is stabilised using a circular steel plate (38 mm in diameter and 31 mm thick) located 21 mm above the burner surface. A vertical translation mechanism was used to provide fine displacement of the burner with respect to the optical components. The flow rates of ethylene and air were measured using rotameters, whose calibration was independently verified in-house by comparison with Bronkhorst EL-Flow mass flow controllers. Pressure measurements were taken immediately downstream of the rotameters to rule out any effect of pressure on the flow measurements. Flames with equivalence ratio of 1.72, 1.90 and 2.15 were studied; in each case, the cold gas velocity at the burner surface was 5.82 cm/s (at 298 K and 1 atm).

The burner used in this work does not have a co-annular flow of air or inert gas to shield the flame. Careful efforts were therefore made to check that the flame was stable and free of radial gradients [25]: this involved performing repeated LII measurements at the centreline of the burner as well as recording radial profiles of peak LII signal. The measured radial LII profile recorded at 15 mm above the burner in the $\phi = 2.15$ flame is shown in Fig. 2. The standard deviation of the measurements is only 1.5 % of the mean over a 17-mm-wide region at the centre of the flame. This seems to suggest that the burner produces flames that are well approximated as one-dimensional at the centreline, despite being narrower than the standard McKenna burner. Interestingly, the flames studied here nevertheless displayed a stronger sooting tendency than ethylene–air flat flames of the same composition studied by other authors. The reasons for this are examined in the discussion section of this paper.

Calibration of the voltage produced by the lock-in amplifier to the soot volume fraction in the flame was achieved by directly measuring the extinction of the diode

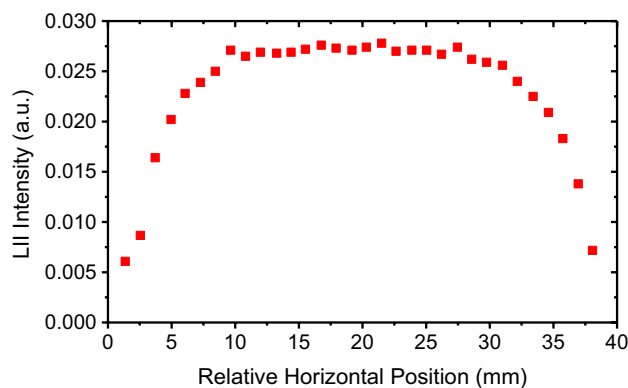


Fig. 2 Prompt LII signals recorded at 15 mm above the burner in the $\phi = 2.15$ flame at a range of radial positions

laser as it is passed through the $\phi = 2.15$ flame at 15 mm above the burner surface. To do this, a lower laser power of 2 W was used (the lowest power at which the laser output power was stable). The transmitted beam was sampled using a reflection from a quartz microscope slide, which was further attenuated by neutral density filters and focused onto a silicon photodiode. Repeated measurements were taken in the presence and absence of the flame. For the purpose of calculating the extinction coefficient, the radial soot distribution was assumed to have a top-hat profile with a diameter of 33 mm.

It was assumed that the extinction coefficient is equivalent to the absorption coefficient of the soot (k_{abs}) [26] which can be related to the soot volume fraction (f_v) using the soot absorption function, $E(m)$ as follows.

$$k_{\text{ext}} \approx k_{\text{abs}} = f_v \frac{6\pi E(m)}{\lambda} \quad (1)$$

There is considerable uncertainty over the value of $E(m)$, and it indeed may depend on soot maturity. A value of $E(m) = 0.3 \pm 0.06$ is suggested by Schulz et al. [23] as being representative of the range of measured values. The soot volume fraction measured by extinction at 15 mm above the burner in the $\phi = 2.15$ flame allows for the calibration of both the photoacoustic soot detection and the LII measurements.

Laser-induced incandescence measurements were taken in the same burner to provide profiles of soot volume fraction to compare with the photoacoustic measurements. The LII measurements were taken using a Nd:YAG laser (1064 nm) with pulse duration of roughly 7 ns. A top-hat spatial profile was formed using a 1-mm-diameter pinhole located 10 cm from the centre of the burner. The laser fluence of the top-hat beam was 480 mJ cm^{-2} . The LII signal emitted at the centreline of the flame was collected on an axis perpendicular to the laser beam using a

photomultiplier tube (Hamamatsu R636-10) with an interference filter centred at 450 nm. Signals were averaged over 64 laser shots, and relative soot volume fraction profiles were obtained by evaluating the peak of the LII temporal profile.

3 Experimental results

Measurements of the photoacoustic signal recorded for flames of three different equivalence ratios at several positions above the burner surface are shown in Fig. 3. A background photoacoustic signal of 0.23 V was measured in the absence of the flame and has been subtracted from each data point. The photoacoustic measurements indicate that the onset of soot formation takes place at 7 mm above the burner surface. A high level of repeatability can be observed in the recorded measurements: the error bars represent the standard deviation calculated from three repeated height translations. A clear trend of increasing soot volume fraction can be observed as the flame becomes richer. Also shown in Fig. 3 is an arrow indicating that visible radiation is first observed in the flame at a height of 5.5 mm above the burner surface. This threshold was determined by recording images of the flame using a digital SLR camera (Nikon) and plotting the intensities of the red pixels as a function of height above burner.

A thorough evaluation of the photoacoustic technique requires comparison to independent reference measurements performed in the same burner. Figure 4 shows the comparison of the photoacoustic measurements with those recorded under the same burner conditions using LII with a 1064-nm pulsed Nd:YAG laser and a detection wavelength of 450 nm. The results of both techniques have been calibrated using the extinction measurements made with the same 808-nm diode laser (accordingly the PA and LII measurements have the same value at HAB = 15 mm in the richest flame condition). The results obtained using the photoacoustic technique are in close agreement with those gained from LII with respect to the shapes of the profiles and the relative signal levels between the three flame conditions. Both techniques show a clear threshold at 7 mm above the burner surface where soot is first detected. This agreement seems to indicate that the absorption (and hence acoustic signal) is due to the particulate soot matter within the flame and not due to broadband absorption from large aromatic species that are formed slightly lower in the flame. The small increase in photoacoustic signal level close to the burner surface is due to burner surface being heated by the far field of the laser beam. The close agreement between the results indicates that any perturbation of the flame by the high-power cw laser appears to have little effect on the measured soot distribution.

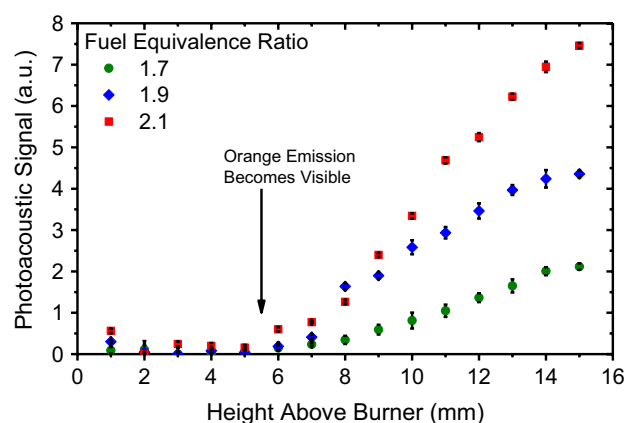


Fig. 3 Soot profiles obtained in an ethylene–air flat flame using photoacoustic detection. Error bars represent 1 standard deviation

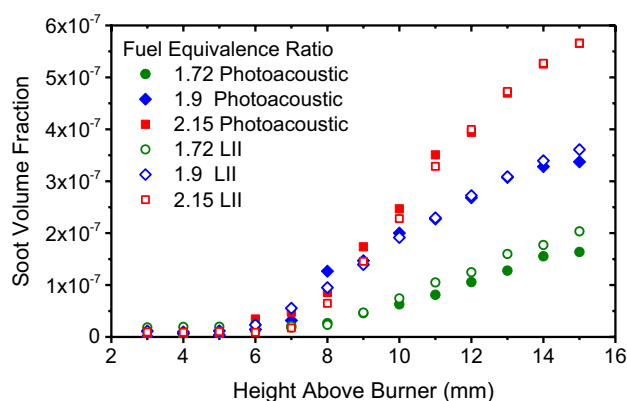


Fig. 4 Comparison of soot profiles obtained using photoacoustic and LII detection methods

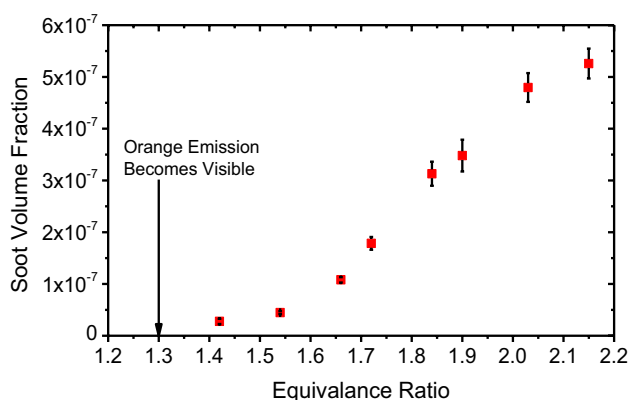


Fig. 5 Soot volume fraction measured photoacoustically at a range of equivalence ratios measured 14 mm above the burner surface

The photoacoustic signal was measured for a wider range of equivalence ratios at 14 mm above the burner

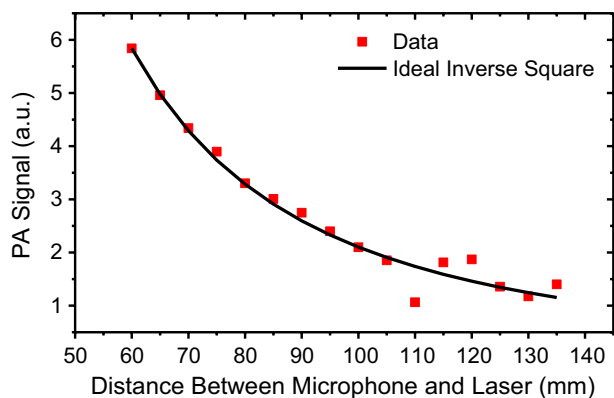


Fig. 6 Results of translating the microphone away from the burner with a model inverse-square law drop off from the initial value

surface, and the results are shown in Fig. 5. This shows the expected trend of increasing soot volume fraction towards higher equivalence ratio. The photoacoustic measurements indicate a threshold for the onset of soot formation at a fuel equivalence ratio of approximately 1.4. This surprisingly low threshold for soot formation is discussed in detail in a later section. Also shown in Fig. 5 is an arrow indicating that visible orange emission is first observed at an equivalence ratio of about 1.3. The appearance of visible emission both in slightly less rich flames and at somewhat lower height above burner than the onset of soot formation as determined by laser measurements is an interesting observation. The main purpose here, however, is to present the technique of photoacoustic soot measurement and to show the close agreement with LII.

The sensitivity of the photoacoustic soot measurements was estimated by taking repeated measurements at 3-s interval over a period of 150 s in the absence of the flame. The standard deviation of these repeated measurements was 0.0224 V. A limit of detection of 5 ppb of soot was thus calculated as three times the standard deviation of the blank measurement. The detection limit is therefore about 1 % of the maximum soot volume fraction measured in the flames studied here.

In order to confirm that the photoacoustic signal detected by the MEMS microphone had originated from the interaction of the laser with the flame, and not due to any ambient photoacoustic effects, the position of the microphone was translated on a horizontal axis perpendicular to the laser beam axis and signals were recorded at each location as described above. The results from this test are shown in Fig. 6. The recorded signals follow an inverse-square relationship with distance from the source of the sound at the centre of the burner. This provides further evidence that the photoacoustic signal is generated solely within the flame.

4 Discussion

In introducing photoacoustic soot measurement, it is worthwhile to consider how various parameters may influence the technique. The laser-heated soot particles can be expected to thermally equilibrate with the local gas on a timescale that is very fast compared to the modulation period of 100 μ s. The laser therefore causes an increase in the local gas temperature along its length, where soot is present. The timescale for heat transfer away from this laser-heated zone, due to conduction and gas flow, is much slower. Modulation of the laser intensity at 10 kHz causes the temperature in the laser-heated zone to vary at the same frequency, leading to the photoacoustic signal. A number of factors may affect the signal generation process in ways that have not been studied in detail in this demonstration of the technique. These include, amongst others, the laser spatial profile, the flame temperature, the ambient pressure and the speed of sound in the surrounding gas. The effect of such issues on the LII technique has been the subject of previous research [23], and similar investigation would be required to fully assess the applicability of photoacoustic soot measurement.

It has been noted that the modulation amplitude for these experiments was limited by the bandwidth of the current controller and laser system. This leads to the possibility of performing photoacoustic soot detection with a much lower power diode laser and/or achieving greater sensitivity by increasing the modulation amplitude. The relationship between the amplitude of laser modulation and the photoacoustic signal requires further investigation, but the simplest possible assumption would be a linear proportionality. This would mean that similar sensitivity to that reported here could be achieved using a 130-mW diode laser modulated between zero and maximum power, which would significantly enhance the simplicity and practicality of the technique.

Various factors might be responsible for the slight differences in the soot volume fraction profiles recorded by the two techniques shown in Fig. 4, including a deviation of about 5 % for some of the measurements in the $\phi = 1.72$ flame. For example, it should be noted that photoacoustic soot detection is effectively a path-integrated technique and the signal will be generated wherever soot is present along the beam path. The flame is one-dimensional at the centreline, but minor differences in the radial soot profile at the periphery could potentially have a minor influence on any path-integrated technique. The distance from the source of sound to the microphone differs slightly along the pathlength, and the effect of this on the signal generation process may merit further investigation. Nevertheless, the one-dimensional nature of this measurement technique

should not be viewed as a critical limitation since this is an inherent feature of absorption spectroscopy, which has found very widespread application to combustion diagnostics [27, 28]. Tomographic methods are sometimes used to extract spatially precise information from absorption measurements [29, 30], and it is possible that similar approaches could also be applied to photoacoustic data.

The lock-in amplifier time constant of 3 s and signal averaging time of 10 s were chosen because the measurements were being taken in a stable laminar flame. The operating principle of the lock-in amplifier requires the time constant to be many times greater than the period of the laser modulation waveform. Further work would be required to assess the feasibility of performing measurements with higher temporal resolution; increased modulation amplitude may help to allow faster measurements to be made. Whilst this may well allow the study of time-dependent flame behaviour, we make no claim that the technique in its present configuration could be capable of resolving the timescales and length scales of relevance in turbulent flames. Another feature of practical combustion systems is a high level of ambient sound. The applicability of photoacoustic soot measurements in such noisy environments is yet to be tested.

Absorption of laser light by gas-phase species may be another source of potential uncertainty in photoacoustic soot measurement. As described above, the photoacoustic signal was measured in the absence of the flame and the background signal (which is thought to arise largely from laser heating of the beam dump) was subtracted from the flame measurements. Absorption by gas molecules in the flame could nevertheless act as a source of interference to the photoacoustic measurement. Large aromatic structures may possibly exhibit weak absorption even at wavelengths as long as 808 nm and thus make a small contribution to the photoacoustic signal. This effect could be minimised by using a longer excitation wavelength to make absorption by aromatic species less likely.

As described above, the soot profiles recorded both by photoacoustic measurement and by LII have been calibrated by an extinction measurement. Calibration of soot volume fraction measurements by extinction is fairly widespread in the recent literature [9, 31], but some aspects deserve further discussion. The uncertainty in the value of $E(m)$ has already been mentioned and has an influence on the absolute accuracy of the calibration. Additionally, the particle size and physical properties of soot may change as a function of height above burner. In particular, a variation of $E(m)$ with vertical position has been noted in ethylene–air flat flames by other authors [32, 33]. Since both the prompt LII and the photoacoustic measurement generate a signal that is dependent on the absorption of laser light by soot, such variation in $E(m)$ may introduce experimental

errors in each technique. A wider variation of physical properties would be expected when comparing soot in different types of flames, in engine exhausts and in the atmosphere. The photoacoustic technique would therefore require specific calibration for any such applications.

An interesting feature of the experimental results is that the soot volume fractions are considerably higher than those previously observed on McKenna burners under equivalent conditions [31, 34]. The threshold equivalence ratio for soot formation in our flames is also much lower. The reasons for this discrepancy were studied by using a second burner with a diameter of 64 mm. This burner consists of a water-cooled brass plate drilled with capillary holes [35] instead of a porous plug. A steel plate (64 mm wide and 34 mm high) was located 21 mm above the burner surface. The $\phi = 1.72$ flame was tested on this burner with the flow rates scaled to achieve the same cold gas velocity. It was visibly apparent that the soot volume fraction was much lower in the larger burner, despite having the same feed gas composition. The gas temperature was measured at 7 mm above each burner at the centreline of the flame using an R-type thermocouple with bead diameter 0.5 mm (Omega P13R-020-8). The temperature was about 100 K lower for the narrower burner, which may provide an explanation for the higher rate of soot formation. The gas temperature was also measured near to the stabilisation plate in each burner, and again the temperature was lower in the narrower burner. This may indicate that heat transfer to the stabilisation plate could play a role in determining the temperature profile and thus the soot volume fraction in this type of flame, and we intend to study this effect further in future.

5 Conclusions

We have demonstrated the use of a simple, easy to implement, photoacoustic technique for in situ measurement of soot profiles in a porous-plug flat-flame burner. The photoacoustic measurements compare well to those made using the well-established LII technique, producing repeatable measurements across a range of flame conditions. The simplicity and low cost of photoacoustic soot detection using fibre-coupled cw-diode lasers may make it an attractive alternative for certain applications where the degree of spatial resolution required does not preclude path-integrated measurement techniques. There is scope to improve the technique using a laser capable of achieving a higher modulation depth at the required frequency. This may permit the same measurements to be made at far lower average power and would therefore allow the use of more standard diode lasers that are widely used for combustion diagnostics.

Acknowledgements We would like to acknowledge Dr. Walter Lubeigt, Dr. Ralf Bauer, Dr. Pascale Desgroux and Prof. Clemens Kaminski for the loan of equipment and useful discussions. Gordon Humphries and Jaclyn Dunn were supported by doctoral training grants from the UK Engineering and Physical Sciences Research Council (EPSRC).

Open Access This article is distributed under the terms of the Creative Commons Attribution 4.0 International License (<http://creativecommons.org/licenses/by/4.0/>), which permits unrestricted use, distribution, and reproduction in any medium, provided you give appropriate credit to the original author(s) and the source, provide a link to the Creative Commons license, and indicate if changes were made.

References

1. T.C. Bond, S.J. Doherty, D.W. Fahey, P.M. Forster, T. Berntsen, B.J. DeAngelo, M.G. Flanner, S. Ghan, B. Kärcher, D. Koch, S. Kinne, Y. Kondo, P.K. Quinn, M.C. Sarofim, M.G. Schultz, M. Schulz, C. Venkataraman, H. Zhang, S. Zhang, N. Bellouin, S.K. Guttikunda, P.K. Hopke, M.Z. Jacobson, J.W. Kaiser, Z. Klimont, U. Lohmann, J.P. Schwarz, D. Shindell, T. Storelvmo, S.G. Warren, C.S. Zender, *J. Geophys. Res. Atmos.* **118**, 5380 (2013)
2. G. Oberdörster, A. Maynard, K. Donaldson, V. Castranova, J. Fitzpatrick, K. Ausman, J. Carter, B. Karn, W. Kreyling, D. Lai, S. Olin, N. Monteiro-Riviere, D. Warheit, H. Yang, *Part. Fibre Toxicol.* **2**, 8 (2005)
3. H. Wang, *Proc. Combust. Inst.* **33**, 41 (2011)
4. P. Lindstedt, *Symp. Combust.* **27**, 269 (1998)
5. L.A. Melton, *Appl. Opt.* **23**, 2201 (1984)
6. T. Lehre, B. Jungfleisch, R. Suntz, H. Bockhorn, *Appl. Opt.* **42**, 2021 (2003)
7. B. Quay, T.-W. Lee, T. Ni, R.J. Santoro, *Combust. Flame* **97**, 384 (1994)
8. B. Axelsson, R. Collin, P.-E. Bengtsson, *Appl. Opt.* **39**, 3683 (2000)
9. P. Desgroux, X. Mercier, B. Lefort, R. Lemaire, E. Therssen, J.F. Pauwels, *Combust. Flame* **155**, 289 (2008)
10. S. De Iuliis, F. Cignoli, G. Zizak, *Appl. Opt.* **44**, 7414 (2005)
11. D.R. Snelling, F. Liu, G.J. Smallwood, Ö.L. Gülder, *Combust. Flame* **136**, 180 (2004)
12. A. Elia, P.M. Lugarà, C. Di Franco, V. Spagnolo, *Sensors (Basel)* **9**, 9616 (2009)
13. A.G. Bell, *Am. J. Sci. series 3* **20**, 305 (1880)
14. R.W. Terhune, J.E. Anderson, *Opt. Lett.* **1**, 70 (1977)
15. J. Hodgkinson, R.P. Tatam, *Meas. Sci. Technol.* **24**, 012004 (2013)
16. A. Petzold, R. Niessner, *Appl. Phys. B Laser Opt.* **63**, 191 (1996)
17. H.A. Beck, R. Niessner, C. Haisch, *Anal. Bioanal. Chem.* **375**, 1136 (2003)
18. R. Bauer, G. Stewart, W. Johnstone, E. Boyd, M. Lengden, *Opt. Lett.* **39**, 4796 (2014)
19. A. Miklós, P. Hess, Z. Bozóki, *Rev. Sci. Instrum.* **72**, 1937 (2001)
20. A.G. Howard, D.A. Greenhalgh, *Anal. Chim. Acta* **106**, 361 (1979)
21. K. Tennal, G.J. Salamo, R. Gupta, *Appl. Opt.* **21**, 2133 (1982)
22. A. Rose, G.J. Salamo, R. Gupta, *Appl. Opt.* **23**, 781 (1984)
23. C. Schulz, B.F. Kock, M. Hofmann, H. Michelsen, S. Will, B. Bougie, R. Suntz, G. Smallwood, *Appl. Phys. B* **83**, 333 (2006)
24. International Sooting Flame Workshop, www.isfworkshop.org/forums/
25. J. Dunn, PhD Thesis, University of Strathclyde. (2014)
26. R.J. Santoro, H.G. Semerjian, R.A. Dobbins, *Combust. Flame* **51**, 203 (1983)
27. M.G. Allen, *Meas. Sci. Technol.* **9**, 545 (1998)
28. R.K. Hanson, *Proc. Combust. Inst.* **33**, 1 (2011)
29. P. Wright, N. Terzija, J.L. Davidson, S. Garcia-Castillo, C. Garcia-Stewart, S. Pegrum, S. Colbourne, P. Turner, S.D. Crossley, T. Litt, S. Murray, K.B. Ozanyan, H. McCann, *Chem. Eng. J.* **158**, 2 (2010)
30. W.W. Cai, C.F. Kaminski, *Appl. Phys. Lett.* **104**, 034101 (2014)
31. R. Hadeef, K.P. Geigle, W. Meier, M. Aigner, *Int. J. Thermal Sci.* **49**, 1457 (2010)
32. F. Migliorini, K.A. Thomson, G.J. Smallwood, *Appl. Phys. B* **104**, 273 (2011)
33. H. Bladh, J. Johnsson, N.E. Olofsson, A. Bohlin, P.E. Bengtsson, *Proc. Combust. Inst.* **33**, 641 (2011)
34. H. Bladh, N.E. Olofsson, T. Mouton, J. Simonsson, X. Mercier, A. Faccinetto, P.E. Bengtsson, P. Desgroux, *Proc. Combust. Inst.* **35**, 1843 (2015)
35. I.S. Burns, J. Hult, G. Hartung, C.F. Kaminski, *Proc. Combust. Inst.* **31**, 775 (2007)